Heliyon 10 (2024) e25128

Contents lists available at ScienceDirect

Heliyon

journal homepage: www.cell.com/heliyon

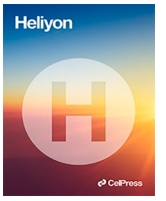

Research article

Three-year black carbon aerosol synthesis over a pristine location surrounded by hillocks in Haryana state, India

P.C.S. Devara [a,*], M.P. Raju [b], S.M. Sonbawne [c], K. Vijayakumar [d]

[a] Centre of Excellence in Ocean-Atmospheric Science and Technology (ACOAST) & Environmental Science and Health (ACESH) & Air Pollution Control (ACAPC), Amity University Haryana (AUH), Gurugram, India
[b] Amity Institute of Environmental Sciences, Amity University Uttar Pradesh (AUUP), Noida, India
[c] Indian Institute of Tropical Meteorology (IITM), Pune, India
[d] Humanities and Sciences Department, Annamacharya Institute of Technology and Sciences, Rajampet, AP, India

ARTICLE INFO

Keywords:
BC aerosols
Aethalometer
Light absorption
Rural environment
Characteristic pollutants
Boundary layer

ABSTRACT

The three-year Black Carbon (BC) aerosol measurements made during 2020, 2021, and 2022 over a rural location, namely, Panchgaon, surrounded by Aravali hillocks (elevation of about 400–600 m) have been analyzed with an aim to determine their optical and radiative characteristics, seasonal and long-term variations in mass concentration. The affinity between these parameters and associated pollutants and planetary boundary layer height (PBLH), affected by the orography, to delineate their role in mass concentration changes with time have been investigated. The coincident OPAC (Optical Properties of Aerosols and Clouds) Model-derived aerosol optical depth (AOD), and single scattering albedo (SSA) have been compared with the observed BC mass concentration, and also with synchronous satellite measurements. The year-to-year variability analysis of the data reveals that the rate of increase of BC concentration is high. The variability was low due to the reasons explained. It implies that the year-to-year variability in BC concentration at the study site depends on the source strength modulated by the valley-driven meteorology. Added, the percentage departures of BC concentration show positive values (higher concentration) during morning and evening hours, which could be due to more anthropogenic activities while it shows negative values during afternoon hours and lower boundary layer heights. The force exerted by the radiation due to BC aerosols at the bottom of the atmosphere (BOA), and in the atmosphere (ATM) are almost equal in magnitude and negative, while that at the top-of-the-atmosphere (TOA) is smaller and positive, indicating that BC aerosols in the study region cools the atmosphere at the BOA and warms the ATM and TOA, which indirectly reveals the dominant role of long-range transport phenomenon at higher levels as compared to the surface level.

1. Introduction

BC aerosol is the dominant light absorbing particulate matter in the atmosphere, emitted by incomplete combustion of both anthropogenic (e.g., diesel engines) and natural (e.g., wildfire) origins. India is currently the second-largest emitter of BC in the world. Several review articles on the current status and future scope of BC aerosol have been published in the literature [1,2]. Among aerosol

* Corresponding author.
E-mail address: pcsdevara@ggn.amity.edu (P.C.S. Devara).

https://doi.org/10.1016/j.heliyon.2024.e25128
Received 26 August 2023; Received in revised form 16 December 2023; Accepted 21 January 2024
Available online 26 January 2024

chemical constituents, BC is the most potent climate forcing agent with a radiative forcing (RF) around ~65 % of that of CO_2 [3], while BC is a source of warming on a global/hemispheric/continental/regional scale, it has adverse effects on air quality and human health. Assessing the sources of BC, their emissions and spatial distribution are very important both for policy making and climate studies. In the Asian regions, the residential, industrial, power and transportation emission rates of BC aerosols during different seasons play in a variety of ways in the formation and development of clouds, precipitation, and hence climate [4,5]. Moreover, these short-lived climate drivers cause upward motion anomalies in the atmosphere [6] that result in changes in dynamic and hydrologic fields [7, 8]. The potential sources and processes involved in carbonaceous aerosols and their effects on climate sustainability and health hazards have been reviewed by many researchers in the literature [9–11]. Due to the absence of long-term regionally representative atmospheric BC data, climate models use emission estimates derived from fuel consumption inventories as inputs for simulation of BC mass density and radiative forcing. Hence, there are many uncertainties and errors in the BC aerosol estimations [10,12]. In view of these projections and uncertainties, model outputs of BC mass densities using these emission estimates need to be urgently constrained by high space-time resolution multi-platform atmospheric measurements in India. The crop-residue burning in India during April–May and October–November, especially in Punjab, Haryana and Uttar Pradesh, and its impact on air quality and human health (respiratory and cardiovascular) has been studied by numerous researchers [3,11,13]. Recent studies at local, urban, and regional scales have shown that high levels of BC and $PM_{2.5}$ emissions from crop residue burning affect air quality not only in India but also across South Asia, due to long-range transport of transboundary pollution [14,15]. Exposure to BC aerosols has also been linked to adverse cardiovascular and respiratory effects in humans [16]. In the light of these strong evidence, a National Carbonaceous Aerosol Programme (NCAP) of the Indian Network for Climate Change Assessment (INCCA) was launched way back in March 2011 by the Government of India to monitor and mitigate the BC emissions. Subsequently, a number of new standalone and multi-lateral collaborative research programs have been developed [17].

In the present work, we report the results of a three-year-long measurements of BC aerosols made with a next-generation Magee Scientific Aethalometer model AE33 during 2020–2022 over a typical rural site, namely, Panchgaon, a valley-like station enveloped by Aravalli hillocks. Some preliminary results observed over this station have been published elsewhere [18]. The present paper deals with the seasonal variation, emphasizing scavenging phenomenon during monsoon and impact of local boundary layer height during winter seasons, besides the radiative forcing exerted by the BC aerosols and covariations between the mass concentrations of BC and coincident characteristic pollutants present and meteorology over the study site.

2. Materials and methods

The study site, Panchgaon (28.31°N, 76.90°E, 285 m a.m.s.l.), Haryana State, is a rural location, situated around 50 km from Delhi. The station is surrounded, in northeast direction, by two cities, namely, Gurugram (~24 km) and Manesar (~9.5 km) which possess several small- and large-scale industries, the study site receives pollution whenever the wind blows in the northeast sector. It is about 7 km away from the Delhi-Jaipur National Highway (NH8) in the northeast direction, and is enveloped by Aravalli hillocks of average elevation of about 200 m. Thus, the experimental site has complex topography with valley-like terrain. The site receives pollution due to traffic, particularly during night-time when heavy vehicles play on the NH road. Added, the complex wind pattern induced by the surrounding orography often affects the pollution flow at the study region. It is also observed that the site is influenced by the Thar Desert, located in the northeast direction, and receives dust pollution through long-range transport process. Thus, although the site is primarily a rural station with sparse residential buildings, population, and vegetation fields, it poses sporadic pollution due to the above-mentioned natural and anthropogenic activities. The aethalometer used in this study has been equipped with a dehumidifier. Plus, the necessary maintenance and periodic calibration checks have been carried out since its installation. This instrument is fully automatic and uses a continuous filtration of ambient aerosols. It measures BC mass concentration round-the-clock in the wavelength range of 370–950 nm. The BC mass concentration is calculated from the rate of change of attenuation of light from an LED source used in the instrument. More details of the experimental station, description of the Aethalometer and accuracies involved in the estimation of BC data are available elsewhere [19–22]. The density of BC datasets that have gone into the different parameter evaluation and model calculations are presented in Table 1. It may be noted that data have been recorded almost every day during the study period, except for a few days due to either power failure or maintenance work. Table 1 presents the number of days on which measurements of BC were conducted in each month during the study period.

Table 1
Number of data points (daily means) available in each month.

	Jan	Feb	Mar	Apr	May	Jun	Jul	Aug	Sep	Oct	Nov	Dec
2020	11	29	31	25	30	30	27	29	22	22	30	27
2021	25	25	31	22	29	10	0	19	30	30	29	28
2022	31	22	31	29	14	30	31	31	28	31	25	16

The daily mean values of BC aerosol data are used for the analyses of seasonal variation and trends, radiative forcing models and satellite data analyses. The synchronous columnar aerosol optical depth (AOD), and single scattering albedo (SSA) from MODIS (Moderate Resolution Imaging Spectroradiometer); Ozone (O_3) from OMI (Ozone Monitoring Instrument) Aura satellite; columnar water vapor (CWV) from AIRS (Atmospheric Infrared Sounder) satellite and Planetary Boundary Layer Height (PBLH) data from MERRA-2 (Modern Era Retrospective analysis for Research and Applications, Version 2) model re-analysis data, and $PM_{2.5}$ from CPCB (Central Pollution Control Board) have also been analyzed to determine their affinity with observed BC mass concentration variations.

3. Results and discussion

3.1. Time series analysis of BC and associated parameters

Fig. 1 depicts the monthly mean variations in BC, $PM_{2.5}$, AOD, SSA, CWV, O_3, temperature (T), relative humidity (RH), wind speed (WS) and PBLH over Panchgaon, a rural station in Manesar (285 m a.m.s.l.), from January 2020 to December 2022. Some gaps observed in the BC and SSA plots are due to the non-availability of data due to some technical problems and unfavorable sky conditions. BC concentration was observed to be in the range of 0.29–10.02 μg/m^3 with an annual mean of 4.21 ± 1.93 μg/m^3, 4.02 ± 2.30 μg/m^3, and 3.94 ± 2.21 μg/m^3 during 2020, 2021, and 2022, respectively. It may be noted here that the lower values of BC during 2022 are majorly due to data gaps due to instrument maintenance issues. Though Panchgaon is basically a pristine region, higher values of BC are normally observed during winter months, which could be due to several factors. High demand of solid fuels for heating, such as coal, wood, and solid waste contribute to the release of BC particles into the atmosphere. Also, stable atmospheric conditions during winter season, such as low wind speeds and lower-level temperature inversions trap the carbonaceous aerosol particles below the boundary layer leads to high BC concentrations. Such conditions favor the accumulation of BC aerosols near the surface [23]. As the winter transitions into summer, BC levels may remain relatively high. This could be attributed to the dust particles suspended in the air due to dry and windy conditions, and also due to long-range transport of crop-residue burning activity in the adjoining regions of the study site. The relatively lower BC concentration observed during winter months (December 2021) (2.50 ± 0.39 μg/m^3) could be attributed to increased wind speed and atmospheric mixing, making it easier to disperse the pollutants. The

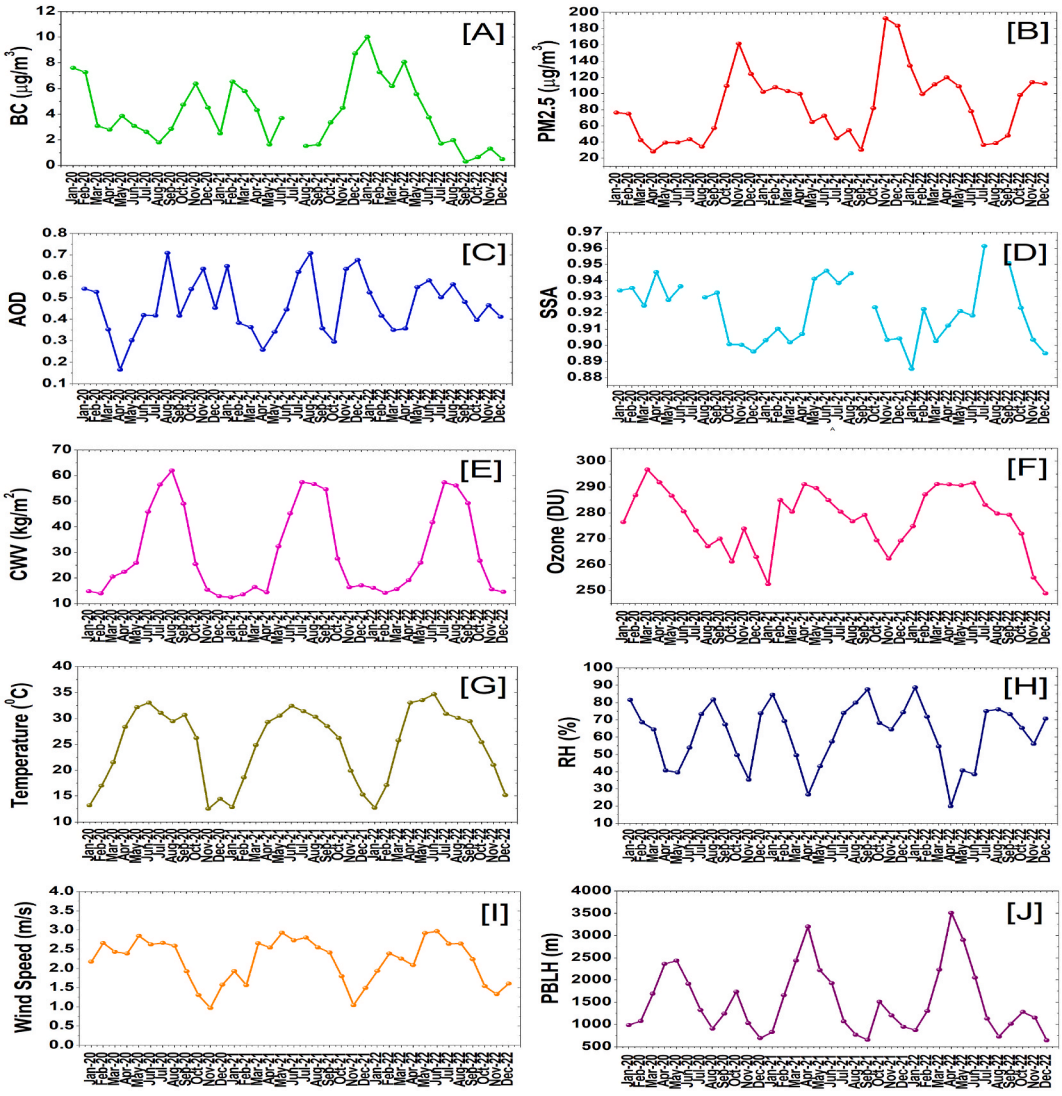

Fig. 1. Covariations between concurrent BC [A], $PM_{2.5}$ [B], AOD [C], SSA [D], CWV [E], Ozone [F], T [G], RH [H], WS [I] and PBLH [J] during the study period of 2020–2022. The solid curve indicates monthly mean variation of each parameter during the study period.

minimum values of BC concentration during the monsoon months (June–September) are due to the well-known cloud- and rain-scavenging processes. Enhancement in BC concentration immediately from the beginning of post-monsoon months (October and November) is due to biomass/crop-waste [24,25]/Parali [26] burning activity in and around the experimental site. Wind direction, precipitation and air mass movements can also affect the transport and dispersion of pollutants, potentially leading to lower BC concentrations. Interestingly, the BC concentrations were observed to be highly fluctuating during post-monsoon (October 2022: 0.64 $\pm$ 0.16 μg/m^3, November 2022: 1.31 $\pm$ 0.16 μg/m^3) and winter (December 2022: 0.49 $\pm$ 0.44 μg/m^3). The variations observed in BC concentration during these months depend on multiple factors such as, the post-monsoon period often experience improved meteorological conditions; increased speed and better dispersion, which help mitigating the accumulation of BC pollutants in the atmosphere. It may be noted here that although the observational station is located in proximity to a state highway, due to the majority of the experimental region is covered under thick vegetation resulting in a relatively less polluted or pristine environment.

The results of the analysis revealed that BC exhibits almost a negative correlation initially and subsequently a positive correlation with O_3, $PM_{2.5}$, PBLH, and AOD. Initially, the BC concentration and planetary boundary layer heights (PBLH) are negatively related, as per the normal expectation. Subsequently, this correlation has become weak. This could be due to strong local sources of BC emissions and winds within or near the PBLH. Moreover, there are industrial emissions/crop residue burning occurring at the same time. Thus, the BC concentrations may rise with the PBL due to local emissions. But, as suggested by Tianning et al. [27], the influence of horizontal transport due to strong winds weakens this relationship (turning into positive) between the PBLH and BC. In another case by Petaja et al. [28], enhancement in BC concentration stabilizes the boundary layer height and hence affects the PBLH-BC correlation. Same is the case with Ozone which is positively correlated with PBLH due to heterogeneous reactions and photolysis rates.

There is usually a negative correlation between BC and O3. The positive relationship observed in the present study has been examined and explained on the basis of the work reported by Chang et al. [29]. This suggests that higher BC concentrations are positively correlated with increased values of these variables. BC showed strong correlation (0.56) with $PM_{2.5}$, as BC being a major contributor to $PM_{2.5}$ concentrations through emissions from combustion processes and its ability to absorb and accumulate other particles in the atmosphere. BC exhibits weak correlation with O3 (0.25), and AOD (0.10), potentially due to the complex interplay of various atmospheric factors, heterogeneous spatial distribution of BC sources at the station. However, BC showed a negative correlation with CWV (−0.57), and SSA (−0.43), indicating that higher BC levels are associated with lower CWV and SSA values. This is due

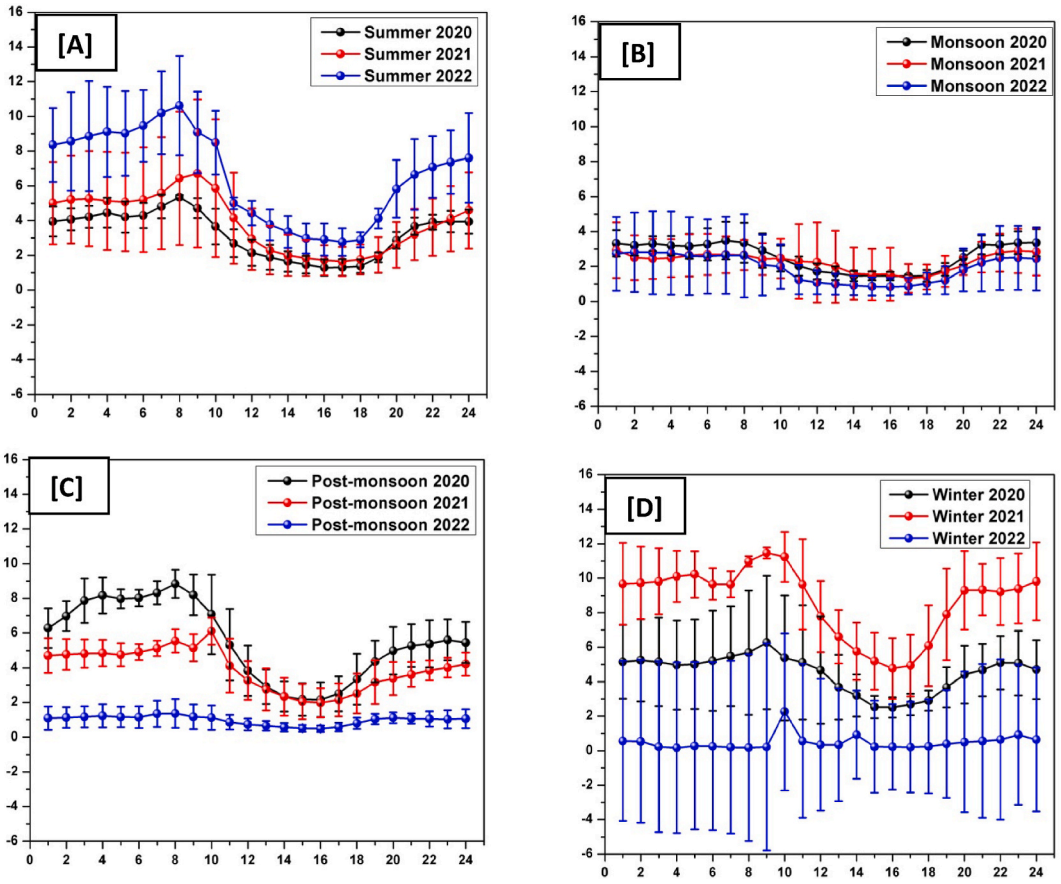

Fig. 2. Seasonal marching of mean diurnal variation of BC mass concentration during summer [A], monsoon [B], post-monsoon [C], and winter seasons during 2020–2022. Vertical bars on each curve represent 1σ deviation from mean.

to suppression of water vapor condensation and increased atmospheric heating, thereby reducing water vapor content, and altering the scattering properties of aerosols. The CWV is high during the monsoon months, implying increased moisture availability. The negative correlation between surface ozone and water vapor indicates that increase in water vapor slows down the ozone production rates, hence its concentration. Moreover, the potential ozone loss due to increase in water vapor occurs due to combination of low temperatures together with elevated water vapor mixing ratios, resulting in activation of liquid sulphate aerosols, leading to ozone depletion [30].

Comparison between AOD and BC leaves an issue of accuracy because they involve different sensing wavelengths. However, the BC measurement involves mainly the absorption component while the AOD and SSA depend on both scattering and absorption [31]. More details of such error analysis have been recently published by Guan et al. [32]. As BC is a significant contributor to $PM_{2.5}$ concentrations, similar variations have been observed in both parameters [33]. Moreover, both showed similar trends. The observed negative correlation between BC and SSA could be explained due to increase in absorption of aerosols faster than the scattering of aerosols [34].

3.2. Time variations of BC mass concentration during different seasons

Fig. 2 shows the season-wise diurnal variation of BC concentration. The solid line indicates the average BC value, and the vertical lines represent the deviation from the mean. The three years' mean of BC concentration exhibits high concentrations during winter (December–February) (6.11 ± 1.44 μg/m^3), followed by summer (March–May) (4.59 ± 1.84 μg/m^3), post-monsoon (October–November) (3.49 ± 1.21 μg/m^3), and monsoon (June–September) (2.26 ± 0.70 μg/m^3) seasons. The BC concentration exhibits a bimodal distribution characterized by two distinct peaks during all the seasons i.e., summer, monsoon, post-monsoon, and winter. The first peak is observed in the morning (summer: 0800–0900 h monsoon: 0700–0800 h, post-monsoon: 0800–1000 h and winter: 0900–1000 h), indicating increased BC levels during this time and the second is observed during late night (summer, monsoon, post-monsoon, and winter: 2300–2400 h), signifies another period of elevated BC concentration. The bimodal pattern of BC distribution suggests a complex interplay of emission sources and atmospheric conditions throughout the day. The three-year seasonal mean of BC contributions was found to be approximately 37 % during winter, followed by 28 % in summer, 21 % in post-monsoon, and 14 % in monsoon. The high standard deviation of BC during winter season (2020–2022) was found to be high, maybe due to the complex topography of the observational site and the resultant microscale meteorological conditions. On the other hand, the arrival of monsoonal rains and enhanced wet deposition of BC particles during monsoon reducing their concentrations resulting in low standard deviation and low BC concentrations. Peaks were observed in the monsoon period due to changes in the planetary boundary layer, vehicular emissions, and local household burning activities [35].

3.3. Percentage departure of hourly mean BC

Studying the departures or deviations in the data series facilitates both qualitative and quantitative information on the time variation of BC mass concentration. The calculation of hourly percentage variation of BC is as explained below:

BC (Percentage Departure) = (((BC instant) - (BC Average)) / (BC Average)) *100

Throughout the study period in Panchgaon, the hourly percentage variation of BC for all the seasons exhibits almost similar pattern as shown in Fig. 3, but within a day, it is found that the BC pollution during daytime significantly higher as compared to nighttime. This is quite interesting to note slow-moving trucks with heavy loads ply on the nearby.

National Highway. It is also clear from the figure that the departures in BC concentrations were positive (indicates more pollution) during daytime. These departures turned into negative from 1000 h and continued up to 2100 h in the night (indicates less pollution)

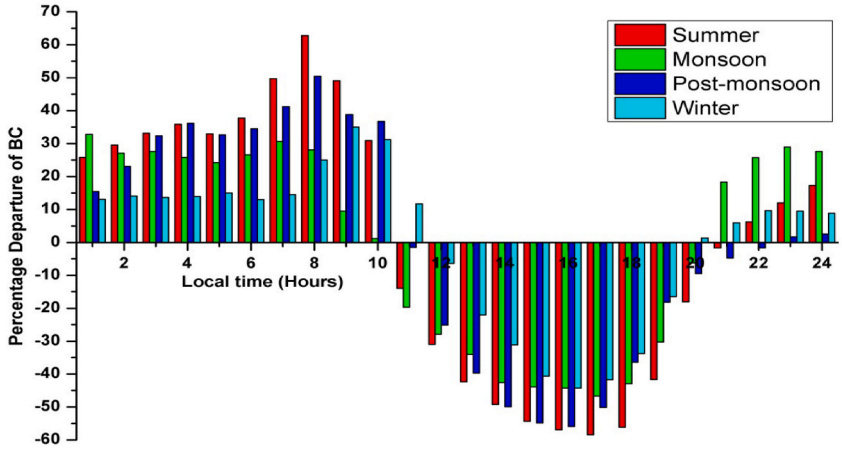

Fig. 3. Time variation of percentage departure of BC concentration during different seasons.

whereas, from 2200 h in the late night to 1000 h in the morning, BC concentration was observed to be consistently higher than that of the annual mean, indicating poor air quality during these hours.

The observed BC variations at the station could be attributed to the combination of anthropogenic activities, meteorological conditions/geographical factors, potential sources, and transport mechanism contributing to BC emissions. The percentage departure of BC was found to be maximum during summer, due to elevated BC level at the station, followed by post-monsoon, monsoon, and winter seasons. The post-monsoon increase could be due to crop residue burning activity. A lower dispersion and more accumulation of BC during winter leads to low BC departure (larger mean) signals compared to other seasons.

3.4. Inter-comparison between AOD and SSA from OPAC model and satellite retrievals

Surface BC concentrations were used in the OPAC model to derive BC optical properties such as AOD, SSA as explained in the paper by Raju et al. [36]. Gogoi et al. [37] have used satellite radiances to retrieve BC mass loading and compared it with the ground-based observations.

Fig. 4 depicts the inter-comparison between AOD and SSA obtained from the OPAC model with satellite derived products. OPAC is a widely used aerosol optical property database that models AOD and SSA values based on different aerosol types. A brief description of the OPAC model, including data retrieval and analysis procedures has been published in the literature [38,39]. The red and black lines represent AOD, blue and purple line indicates SSA derived from OPAC model and Satellite, respectively. The comparison between OPAC-derived AOD and SSA values at 550 nm and satellite products i.e., MODIS and OMI revealed a reasonable agreement. The mean difference between the satellite and modeled values for AOD and SSA was found to be 0.01 and 0.001, respectively, falling within the range of.

Retrieval uncertainty. The average AOD derived from MODIS observations was 0.47, with a peak of 0.72 observed in August 2021 and a low of 0.17 in April 2020. These variations indicate temporal variability in aerosol loading, potentially influenced by seasonal factors or changes in seasonal factors or changes in aerosol sources. On the other hand, SSA derived from OMI satellite observations shows an average value of 0.92 with its maximum of 0.96 observed during August 2020 and minimum of 0.88 in January 2022, these changes in SSA may be due to changes in the scattering properties of aerosols, which could be influenced by different aerosol types during these study periods.

3.5. Monthly mean aerosol direct radiative forcing (ADRF) at Panchgaon during 2020-22

The Santa Barbara DISORT Atmospheric Radiative Transfer (SBDART) model described elsewhere with the RT code published in the literature [40–44] has been used to estimate the aerosol direct radiative forcing (ADRF) values in the present study. While running OPAC using water-soluble, -insoluble, and BC, the mineral transport term is also used for computing the optical properties of aerosols. Thereafter, the SBDART was run for computing the ARF. In Fig. 5, the monthly mean Aerosol Radiative Forcing (ARF) over Panchgaon during 2020, 2021 and 2022 is presented. TOA and ATM forcing exhibit positive ARF, indicating a warming effect. However, the BOA forcing showed negative ARF, suggesting a cooling effect. The three-year mean ARF at TOA, ATM and BOA were determined to be.

13.0 W/m^2, 52.5 W/m^2 and -39.5 W/m^2, respectively. The range of TOA, ATM, and BOA forcing varied from 6.4 to 24.4 W/m^2, 25.1–85.6 W/m^2, and -17.3 to −62.7 W/m^2, respectively. ARF at all the three scenarios (TOA, BOA, ATM) were found to be more during post-monsoon (ON) winter (DJF) months compared to summer (MAM) and monsoon (JJAS). Post-monsoon and winter months at Panchgaon are often associated with crop residue burning; relatively calm atmospheric conditions with reduced vertical mixing, resulting in higher aerosol concentrations and stronger interactions with solar radiation, and leading to increased ARF.

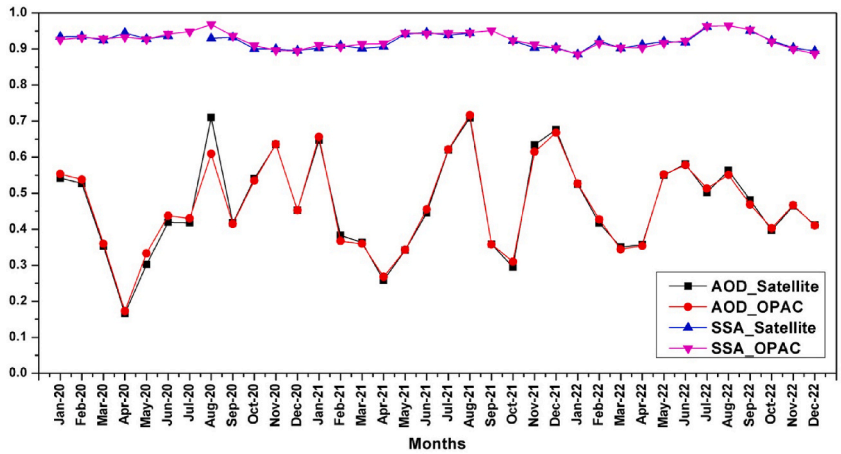

Fig. 4. Comparison of AOD and SSA, derived from OPAC model and satellites during the study period, respectively.

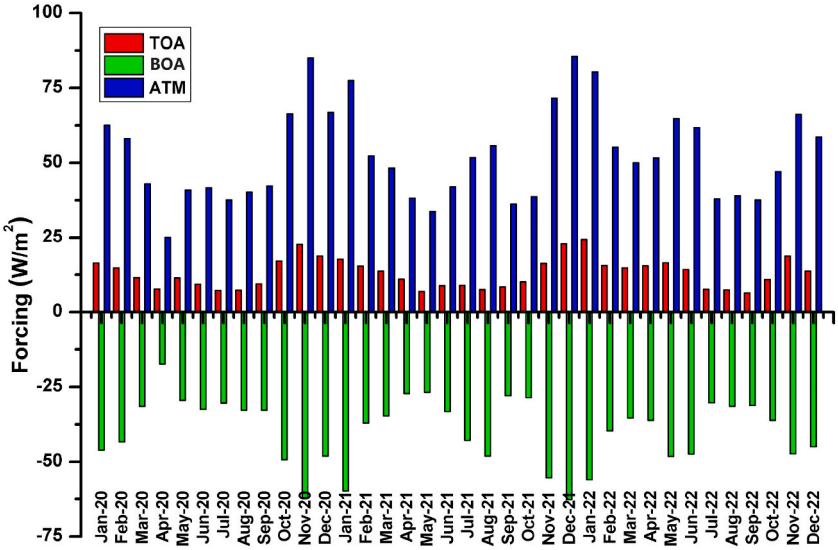

Fig. 5. Direct Radiative Forcing exerted by aerosols at the BOA, ATM and TOA during the study period.

3.6. Airmass back-trajectory cluster analysis

In order to ascertain the pollution source and quantify (per cent) its contribution to the levels observed at the study site during different the study period of three years, namely, 2020, 2021, and 2022, the cluster analysis method of HYSPLIT model analysis has been performed by following the work reported by Draxler et al. [45]. The results are displayed in Fig. 6 (A, B, C). Different colored.

Trajectories indicate the contribution of airmass from different levels of the atmosphere. The number (cluster) and associated percentage (pollution level) given with parenthesis at each trajectory indicates the contribution of the cluster of trajectories to the concentration observed at the experimental site. It is clear from the figure that both land (mostly fine particles) as well as marine (mostly sub-micron particles) air mass travelled in all the three years and contributes to the BC levels at the study site. The airmass trajectory close to the surface contributed maximum, 66 %, 58 %, and 28 % during 2020, 2021, and 2022, respectively. Moreover, the marine air mass contributed maximum around 15 % during 2020 as compared to 2021 (16 %) and 2022 (20 %) during the study period. During the summer months, long-range air masses travel from elevated altitudes, carrying in a mixture of marine and continental/polluted aerosols. The atmospheric loading of BC over the site results from a combination of long-range transport and anthropogenic activity in and around the observation station, such as emissions from transport, industries, and power generators, as explained in our earlier communications [19,28].

Thus, the results obtained over a rural site, enveloped by Aravalli hillocks, employing a multi-spectral aethalometer (AE33 of Magee Scientific) for the period 2020–2022 during COVID-19 and post-COVID-19, have been reported. The departures from mean BC mass concentration yielded both quantitative and qualitative estimates. The BC mass concentration showed an interesting association with surface-level temperature, wind speed, $PM_{2.5}$, Ozone, planetary boundary layer height, and columnar aerosol optical depth, water vapor, and single scattering albedo during the study period. The long-range transport of back trajectory cluster analysis showed contribution of BC aerosols from different sources via characteristic altitudes to the study location.

4. Summary and conclusions

The research work reported in this paper focused on the properties of atmospheric black carbon in a pristine environment at Panchgaon from January 2020–December 2022. In addition to analyzing the temporal variation of BC during different seasons, this study also focused on the ADRF derived from OPAC and SBDART models. The key results of the study are outlined below.

1. During the years 2020, 2021, and 2022, BC concentrations were observed within the range of 0.26–10.02 μg/m3. The annual mean BC concentrations were found to be 4.21 ± 1.93 μg/m^3, 4.02 ± 2.30 μg/m^3, and 3.94 ± 2.21 μg/m^3 for the respective years.
2. The mean BC concentration over a period of three years shows elevated levels during winter with a value of 6.11 ± 1.44 μg/m^3, followed by summer with 4.59 ± 1.84 μg/m^3, post-monsoon with 3.49 ± 1.21 μg/m^3, and monsoon with 2.26 ± 0.70 μg/m^3 seasons.
3. From 1000 h in the morning till 2100 h at night, BC concentrations were observed to be lower than the annual mean. Conversely, from 2200 h in the late night to 1000 h in the morning, concentrations were higher than the annual mean.
4. The average ADRF over a period of three years was calculated to be 13.0 W/m^2 at TOA, 52.5 W/m^2 within the ATM, and −39.5W/m^2 at BOA.

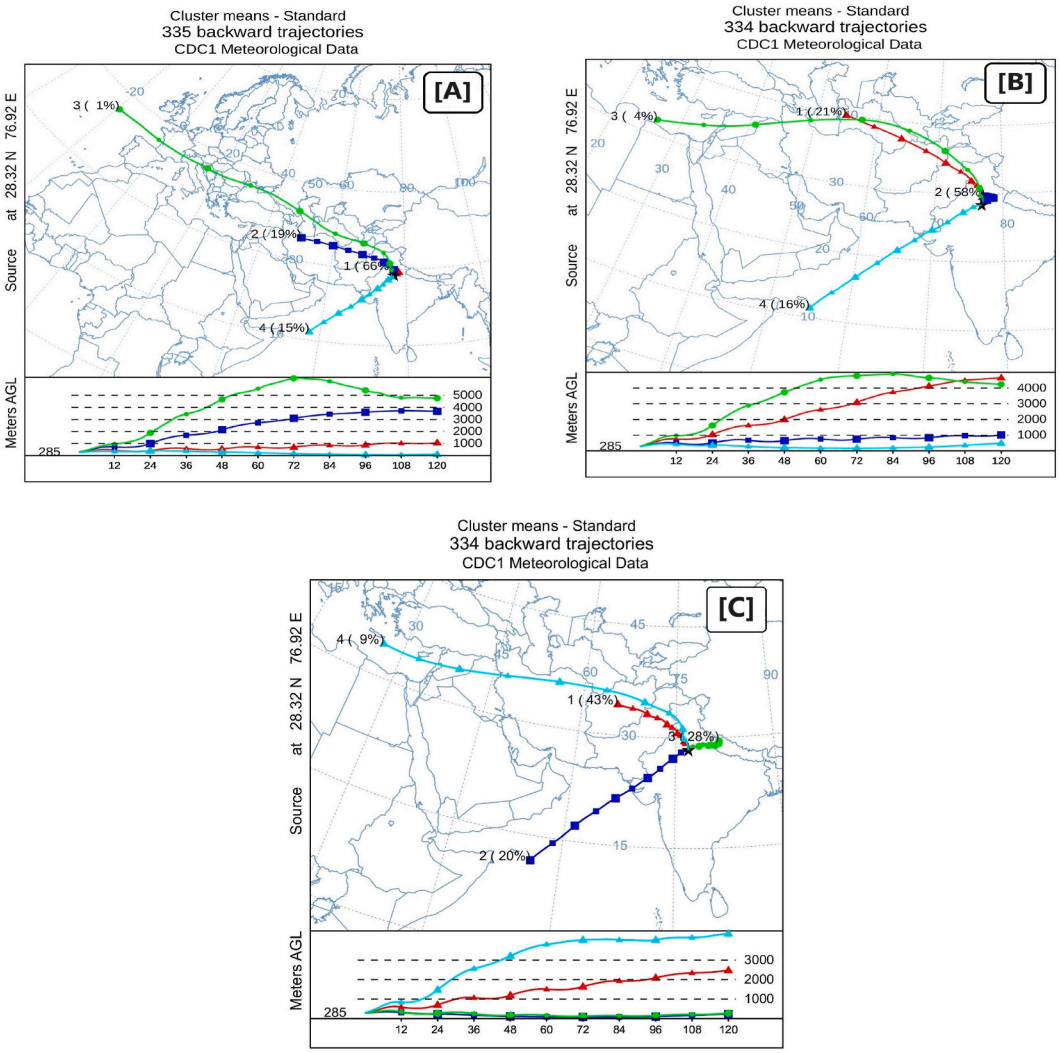

Fig. 6. Cluster-mode analysis of HYSPLIT air mass back-trajectories observed on 2020 [A], 2021 [B] and 2022 [C].

5. BC concentration exhibited, in most cases, initially negative and subsequently positive correlation with PBLH, T, WS, O_3, CWV, SSA, and $PM_{2.5}$ during the study period.
6. BC mass concentration exhibits a positive correlation with O_3 (0.25), $PM_{2.5}$ (0.56), and AOD (0.10), while it shows inverse relationship with PBLH (−0.22), CWV (−0.57), and SSA (−0.43).
7. Ozone was found to correlate positively with PBLH. Negative correlation was found between BC and SSA, and O3 and water vapor.

Author contribution statement

All authors listed have significantly contributed to the development and the writing of this article.

Funding statement

This research did not receive any specific grant from funding agencies in the public, commercial, or not-for-profit sectors.

Ethics statement

No potential conflict of interest was reported by the authors.

Consent to participate statement

The authors declare their consent for the submission.

Consent to publish statement

The authors give their consent for the publication.

Data availability statement

Data will be made available on request.

Declaration of competing interest

The authors declare no conflict of interest.

Acknowledgements

The work reported in this paper was carried out as a part of the joint research collaboration between Amity University Haryana (AUH), Gurugram, India; Indian Institute of Tropical Meteorology (IITM), Pune, Ministry of Earth Sciences (MoES), GoI, New Delhi, India, and Annamayya Institute of Technology & Sciences, Rajampet, Andhra Pradesh (AP), for which the authors are highly grateful to the authorities of the respective Institutions. Thanks, are also due to NOAA Air Resources Laboratory, USA, for HYSPLIT Model Analysis, NASA's MODIS (Moderate Resolution Imaging Spectroradiometer) and Ozone Monitoring Instrument (OMI) Aura satellite products and Central Pollution Control Board (CPCB) datasets, Ministry of Environment, Forests and Climate Change (MoEF&CC), GoI., New Delhi, India. The authors highly appreciate the critical comments and valuable suggestions provided by the Editor and anonymous Reviewers, which helped to improve the scientific content of the original manuscript.

References

[1] A. Rana, Shiguo Jia, Sayantan Sarkar, Black carbon aerosol in India: a comprehensive review of current status and future prospects, Atmos. Res. 218 (1) (2019) 207–230, https://doi.org/10.1016/j.atmosres.2018.12.002.
[2] S.K. Kompalli, S.N.S. Babu, K.K. Moorthy, S.K. Satheesh, M.M. Gogoi, V.S. Nair, V.N. Jayachandran, D. Liu, M.J. Flynn, H. Coe, Mixing state of refractory black carbon aerosol in the South Asian outflow over the northern Indian Ocean during winter, Atmos. Chem. Phys. (21) (2021) 9173–9199, https://doi.org/10.5194/acp-21-9173-2021.
[3] T.C. Bond, S.J. Doherty, D.W. Fahey, P.M. Forster, T. Berntsen, B.J. Deangelo, M.G. Flanner, S. Ghan, B. Kärcher, D. Koch, S.G. Warren, C.S. Zender, Bounding the role of black carbon in the climate system: a scientific assessment, J. Geophys. Res. Atmos. 118 (11) (2013) 5380–5552, https://doi.org/10.1002/jgrd.50171.
[4] M.G. Manoj, P.C.S. Devara, P.D. Safai, B.N. Goswami, Absorbing aerosols facilitate transition of Indian monsoon breaks to active spells, Clim. Dynam. 37 (2011) 2181–2198, https://doi.org/10.1007/s00382-010-0971-3.
[5] E.M. Wilcox, Direct and semi-direct radiative forcing of smoke aerosols over clouds, Atmos. Chem. Phys. 12 (1) (2012) 139–149, https://doi.org/10.5194/acp-12-139-2.
[6] C.A. Randles, V. Ramaswamy, Absorbing aerosols over Asia: a Geophysical Fluid Dynamics Laboratory general circulation model sensitivity study of model response to aerosol optical depth and aerosol absorption, J. Geophys. Res. 113 (2008) D21203, https://doi.org/10.1029/2008JD010140.
[7] S. Menon, J. Hansen, L. Nazarenko, Y.F. Luo, Climate effects of black carbon aerosols in China and India, Science 297 (2002) 2250–2253, https://doi.org/10.1126/science.1075159.
[8] T.J. Wang, B.L. Zhuang, S. Li, J. Liu, M. Xie, C.Q. Yin, Y. Zhang, C. Yuan, J.L. Zhu, L.Q. Ji, Y. Han, The interactions between anthropogenic aerosols and the East Asian summer monsoon using RegCCMS, J. Geophys. Res. Atmos. (2015), https://doi.org/10.1002/2014jd0228.
[9] M. Ni, J. Huang, S. Lu, X. Li, J. Yan, K. Cen, A review on black carbon emissions, worldwide and in China, Chemosphere 107 (2014) 83–93, https://doi.org/10.1016/j.chemosphere.2014.02.052.2014.
[10] U. Paliwal, M. Sharma, J.F. Burkhart, Monthly and spatially resolved black carbon emission inventory of India: uncertainty analysis, Atmos. Chem. Phys. 16 (2016) 12457–12476, https://doi.org/10.5194/acp-16-12457-2016, 2016.
[11] R. Lan, S.D. Eastham, T. Liu, L.K. Norfor, R. Steven, H. Barrett, Air quality impacts of crop residue burning in India and mitigation alternatives, Nat. Commun. 13 (2022) 6537.
[12] T.J. Thorsen, D.M. Winker, R.A. Ferrare, Uncertainty in observational estimates of the aerosol direct radiative effect and forcing, J. Clim. 34 (1) (2021) 195–214, https://doi.org/10.1175/JCLI-D-19-1009.1.
[13] V. Kumar, P.C.S. Devara, V.K. Soni, Multisite scenarios of black carbon and biomass burning aerosol characteristics in India, Aerosol Air Qual. Res. 23 (6) (2023) 220435, https://doi.org/10.4209/aaqr.22043.
[14] T. Ohara, H. Akimoto, J. Kurokawa, N. Horii, K. Yamaji, X. Yan, T. Hayasaka, An Asian emission inventory of anthropogenic emission sources for the period 1980-2020, Atmos. Chem. Phys. 7 (2007) 4419–4444, https://doi.org/10.5194/acp-7-4419-2007.
[15] A. Huggins, E. Hawkins, Transboundary air pollution, Yearbook of International Environmental Law 31 (1) (2020) 65–70, https://doi.org/10.1093/yiel/yvab030.
[16] WHO (World Health Organization), World Health Statistics 2012, World Health Organization, 2012. https://apps.who.int/iris/handle/10665/44844.
[17] S.K. Sharma, R. Chauhan, Climate change research initiative: Indian Network for climate change assessment (NCCA), Curr. Sci. 101 (3) (2011) 309–311.
[18] S.M. Sonbawne, P.C.S. Devara, B.D. Priyanka, Multisite characterization of concurrent black carbon and biomass burning around COVID-19 lockdown period, Urban Clim. 39 (2021) 100929.
[19] P.C.S. Devara, M.P. Alam, U.C. Dumka, S. Tiwari, A.K. Srivastava, Anomalous Features of black carbon aerosols observed over a rural station during diwali festival of 2015, in: Book Titled *Environmental Pollution*, Springer Science, 2017, pp. 293–308, https://doi.org/10.1007/978-981-10-5792-2_24.
[20] J. Sun, W. Zhe, Conghui Xie, Cheng Wu, C. Chun, H. Tingting, W. Qingqing, Zhijie Li, Li Jie, Pingqing Fu, Zifa Wang, S. Yele, 22, Measurement Report: Long-Term Changes in Black Carbon and Aerosol Optical Properties from 2012 to 2020 in Beijing, China, vol. 22, ACP, 2022, https://doi.org/10.5194/acp-22-561-2022, 561–575.

[21] S.M. Sonbawne, S. Fadnavis, K. Vijayakumar, P.C.S. Devara, P. Chavan, Phase-Resolved lockdown features of pollution parameters over an urban and adjoining rural region during COVID-19, Front. Environ. Sci. 10 (2022) 826799, https://doi.org/10.3389/fenvs.2022.826799.
[22] Xu Guan, Naiyue Zhang, Pengfei Tian, Chenguang Tang, Zhinda Zhang, Ligong Wang, Yunshu Zhang, Min Zhang, Yumin Guo, Tao Du, Xianjie Cao, Jiening Liang, Lei Zhang, Wintertime vertical distribution of black carbon and single scattering albedo in a semi-arid region derived from tethered balloon observations, Sci. Total Environ. 807 (2022) 150790. Part 1.
[23] S. Tiwari, P.C.S. Devara, P.B. Sharma, G. Beig, B.S. Murthy, Satellite and model observations of the impact of dust and biomass burning on air quality over a pristine location, International Journal of Geoscience and Remote Science (IJGRS) (2022), https://doi.org/10.36266/IJGRS/103, 2022).
[24] K. Vijayakumar, P.D. Safai, P.C.S. Devara, S. Vijaya Bhaskara Rao, C.K. Jayasankar, Effects of agriculture crop residue burning on aerosol properties and long-range transport over northern India: a study using satellite data and model simulations, Atmos. Res. 178–179 (2016) 155–163, 2016.
[25] A.A. Khan, G. Kalpana, P. Jindal, P.C.S. Devara, C.S. P, Effects of stubble burning and firecrackers on the air quality of Delhi, Environ. Monit. Assess. 195 (2023a) (2023) 1170, https://doi.org/10.1007/s10661-023-11635-6.
[26] A.A. Khan, G. Kalpana, J. Prakhar, J. P C S Devara, S. Tiwari, P.B. Sharma, Demographic evaluation and parametric assessment of air pollutants over Delhi NCR, Atmosphere 14 (2023) 1390, https://doi.org/10.3390/atmos14091390.
[27] Tianning Su, Zhanqing Li, Ralph Kahn, Relationships between the planetary boundary layer height and surface pollutants derived from lidar observations over China, Atmos. Chem. Phys. Discuss. (2018), https://doi.org/10.5194/acp-2018-279.
[28] T. Petäjä, L. Järvi, V.M. Kerminen, A.J. Ding, J.N. Sun, W. Nie, J. Kujansuu, Virkkula, X.Q. Yang, C.B. Fu, S. Zilitinkevich, M. Kulmala, Enhanced air pollution via aerosol-boundary layer feedback in China, Sci. Rep. 6 (2016) (2016) 18998, https://doi.org/10.1038/srep18998.
[29] Yi Chang, Tao Du, Xin Song, Wenfang Wang, Pengfei Tian, Xu Guan, Naiyue Zhang, Min Wang, Yumin Guo, Jinsen Shi, Lei Zhang, Changes in physical and chemical properties of urban atmospheric aerosols and ozone during the COVID-19 lockdown in a semi-arid region, Atmos. Environ. 287 (2022 Oct 15) 119270, https://doi.org/10.1016/j.atmosenv.2022.119270.
[30] Sabine Robrecht, Bärbel Vogel, Jens-Uwe Grooß, Karen Rosenlof, Troy Thornberry, Andrew Rollins, Martina Krämer, Lance Christensen, Rolf Müller, Mechanism of ozone loss under enhanced water vapour conditions in the mid-latitude lower stratosphere in summer 19 (9) (2019) 5805–5833, https://doi.org/10.5194/acp-19-5805-2019.
[31] K. Vijayakumar, P.C.S. Devara, Optical exploration of biomass burning aerosols over a high-altitude station by combining ground-based and satellite data, J. Aerosol Sci. 72 (2014) 1–13, https://doi.org/10.1016/j.j.aerosci.2014.01.008.
[32] Xu Guan, Min Wang, Tao Du, Pengfei Tian, Naiyue Zhang, Jinsen Shi, Yi Chang, Lei Zhan, Min Zhang, Xin Song, Yijia Sun, Wintertime aerosol optical properties in Lanzhou, Northwest China: emphasis on the rapid increase of aerosol absorption under high particulate pollution, Atmos. Environ. 246 (2021) 118081, https://doi.org/10.1016/j.atmosenv.2020.118081.
[33] P.D. Safai, P.C.S. Devara, M.P. Raju, K. Vijayakumar, P.S.P. Rao, Relationship between black carbon and associated optical, physical, and radiative properties of aerosols over two contrasting environments, Atmos. Res. 149 (2014) 292–299.
[34] Pradeep Khatri, Tamio Takamura, Atsushi Shimizu, Nobuo Sugimoto, Observation of Low Single Scattering Albedo of Aerosols in the Downwind of the East Asian Desert and Urban Areas during the Inflow of Dust Aerosols, JGR Atmospheres, 2013, https://doi.org/10.1002/2013JD019961.
[35] P.S. Buchunde, P.D. Safai, S. Mukherjee, M.P. Raju, G.S. Meena, S.M. Sonbawne, K.K. Dani, G. Pandithurai, Seasonal Abundances of Primary and Secondary Carbonaceous Aerosols at a High-Altitude Station in the Western Ghat Mountains, India, Air Quality, Atmosphere & Health, 2019, https://doi.org/10.1007/s11869-021-01097-5.
[36] M.P. Raju, P.D. Safai, K. Vijayakumar, P.C.S. Devara, C.V. Naidu, P.S.P. Rao, G. Pandithurai, Atmospheric abundances of black carbon aerosols and their radiative impact over an urban and a rural site in SW India, Atmos. Environ. 125 (2016) 429–436. www.elsevier.com/locate/atmosenv.
[37] M.M. Gogoi, S.S. Babu, R. Imasu, M. Hashimoto, Satellite (GOSAT-2 CAI-2) retrieval and surface (ARFINET) observations of aerosol black carbon over India, Atmos. Chem. Phys. 23 (2023) 8059–8079, https://doi.org/10.5194/acp-23-8059-2023, 33.
[38] M. Hess, P. Koepke, I. Schult, Optical properties of aerosols and clouds: the software package OPAC, 1998, Bull. Am. Meteorol. Soc. 79 (5) (1998) 831–844, https://doi.org/10.1175/1520-0477(1998)079<0831:OPOAAC>2.0.CO;2.
[39] Pengfei Tian, Naiyue Zhang, Jiayun Li, Xiaolu Fan, Xu Guan, Yuting Lu, Jinsen Shi, Yi Chang, Lei Zhang, Potential influence of fine aerosol chemistry on the optical properties in a semi-arid region, Environ. Res. 216 (2023) 114678, https://doi.org/10.1016/j.envres.2022.114678.
[40] M.P. Raju, P.D. Safai, S.M. Sonbawne, P.S. Buchunde, G. Pandithurai, K.K. Dani, Black carbon aerosols over a high altitude station, Mahabaleshwar: radiative forcing and source apportionment, Atmos. Pollut. Res. 11 (Issue 8) (2020) 1408–1417, https://doi.org/10.1016/j.apr.2020.05.024.
[41] P. Ricchiazzi, S. Yang, C. Gautier, C. D Sowle, SBDART: a research and teaching software tool for plane-parallel radiative transfer in the earth's atmosphere, Bull. Am. Meteorol. Soc. 79 (No. 10) (1998).
[42] Pengfei Tian, Zeren Yu, Chen Cui, Jianping Huang, Chenliang Kang, Jinsen Shi, Xianji Cao, Lei Zhang, Atmospheric aerosol size distribution impacts radiative effects over the Himalayas via modulating aerosol single-scattering albedo, Climate and Atmospheric Science 6 (54) (2023), https://doi.org/10.1038/s41612-023-00368-5.
[43] S. Korkin, A.M. Sayer, A. Ibrahim, A. Lyapustin, A practical guide to writing a radiative transfer code, Comput. Phys. Commun. 271 (2022) 108198, https://doi.org/10.1016/j.cpc.2021.108198.
[44] S.M. Sonbawne, M.P. Raju, P.D. Safai, P.C.S. Devara, Suvarna Fadnavis, A.S. Panicker, G. Pandithurai, Size-separated aerosol chemical characterization over Ny-Ålesund during the Arctic summer of 2010, Sustainable Chemistry for Climate Action (SCCA) 2 (2023) 100016.
[45] R.R. Draxler, G.D. Rolph, HYSPLIT (Hybrid Single-Particle Lagrangian Integrated Trajectory) Model, vol. 11, NOAA Air Resources Laboratory, Silver Spring, MD, 2010, pp. 7815–7875. http://ready.arl.noaa.gov/HYSPLIT.php, 18 (2010),.